ECG gated tomographic reconstruction for 3-D rotational coronary angiography.

Yining Hu, Lizhe Xie, Jean Claude Nunes, Jean Jacques Bellanger, Marc Bedossa, Christine Toumoulin

ECG Gated Tomographic reconstruction for 3-D Rotational Coronary Angiography

Yining HU, Lizhe XIE, Jean Claude NUNES, Jean Jacques BELLANGER, Marc BEDOSSA, Christine TOUMOULIN

Abstract— **A method is proposed for 3-D reconstruction of coronary from a limited number of projections in rotational angiography. A Bayesian maximum a posteriori (MAP) estimation is applied with a Poisson distributed projection to reconstruct the 3D coronary tree at a given instant of the cardiac cycle. Several regularizers are investigated L0-norm, L1 and L2 -norm in order to take into account the sparsity of the data. Evaluations are reported on simulated data obtained from a 3D dynamic sequence acquired on a 64-slice GE LightSpeed CT scan. A performance study is conducted to evaluate the quality of the reconstruction of the structures.**

I. INTRODUCTION

Cardiologists, who are under tremendous time constraints, ask for new advances in angiography imaging techniques to improve both the safety and the efficacy of coronary angiography interventions. Today, the rotational angiography allows to obtain up to 180 projections of the left or right coronary tree during a single injection of contrast under different angles (caudal, cranial, axial). It provides thus a complete range of projections, giving a pseudo 3-D view of the coronary tree with all the structures moving all together but a challenge remains the 3D coronary reconstruction that will provide the ground for a platform dedicated to the planning and execution of percutaneous coronary interventions. Indeed rapid, online 3D coronary reconstruction remains an open problem due to the cardiac motion which is unknown, non-linear and not always regular. Mainly two different approaches have been applied to the reconstruction of coronary in rotational angiography imaging [1]. The first one considers the reconstruction as an inverse problem. Two kinds of methods have been used respectively based on filtered back projection [2] and iterative reconstruction techniques [3-4]. Nevertheless, the presence of the motion leads to consider an ECG gated reconstruction with a very limited number of projections (i.e. associated with the same motion stage). Filtered backprojection methods generally yield unsatisfactory results with many artifacts while iterative reconstruction techniques try to overcome these limitations by using regularization function to incorporate prior information. An alternative consists to first estimate the motion of the coronary arteries throughout the cardiac cycle and performed then a motion compensated reconstruction of the structure at a given phase of the cardiac cycle, using the set of overall projections. This reconstruction is then performed either with iterative [5-6] or filtered back projection [7-8] methods. This kind of method involves applying, as modeling techniques, computer vision methods to extract the coronary tree on all the images of the sequence and determine the 4D motion vector field (3D+T).

We present a modified version of an ECG gated statistic based iterative reconstruction method [3]. We first investigated a technique for accelerating the computation of conebeam forward and backward projections (section II.A) and evaluated then three regularization functions (respectively L0,L1 and L2 norm) to take into account the sparsity of the data(section II.B). The optimization process relies on a separable paraboloidal surrogates (SPS) algorithm (Section II.C). Preliminary results are given on simulated data in section III.

II. METHOD

A. Projection Matrix

The computation of forward and backward projections represents the basic stages of tomographic reconstruction algorithms. Several interpolation methods have been proposed (that are pixel, ray or distance driven), which provide some compromise between computational complexity and accuracy [9]. They nevertheless remain highly time consuming. One way to reduce this computation time consists in pre-storing the projection matrix. This is often used in conventional 2D tomography reconstructions. However in the case of the 3D reconstructions, the size of the matrix becomes too large. Thus, if we consider a volume of size $256 \times 256 \times 256$ voxels, 80 image projections of size 256×256 pixels corresponding to a rotational acquisition with an angular coverage of RAO60^o to LAO60^o and a fan angle of $2\pi/3$, then the size of the matrix amounts to 7864320×16777216 The fact to deal with sparse objects does not simplify its computation. Nevertheless, numerical simplification can be considered if the matrix is symmetric.

This work is supported by the French agency for research (ANR Mesange N^{o}09FA388-01) and by the National Basic Research Program of China (#2010CB732503).

Y. Hu and L. XIE are with the Laboratory of Image Science and Technology (LIST), South East University, C-210096 Nanjing, China

J. C Nunes, J.-J. Bellanger, and C. Toumoulin are with the French National Institute for Health and Medical Research (INSERM), U642, Rennes F-35000,France

J. C Nunes, J.-J. Bellanger, M. BEDOSSA, and C. Toumoulin are with the Laboratoire Traitement du Signal et de l'Image (LTSI), Universite de Rennes 1, Rennes F-35000, France.

M. BEDOSSA is with Département de Cardiologie interventionelle, CHU Rennes, 35033 Rennes, France

C. Toumoulin, L. XIE and Y. Hu are also with the Centre de Recherche en Information Biomedicale Sino-Francais (LIA CRIBs), Rennes, F-35000, France.

We can thus separate it into a product of 2 matrices to make possible its storage.

Let consider $\boldsymbol{f}$ the 3D object, $\boldsymbol{b}$ the noisy background image and $\boldsymbol{\theta} = \{\theta_1, \theta_2, \cdots, \theta_M\}$ the device positions (angles), M being the number of considered rotation angles. Then the corresponding projection planes $\boldsymbol{g} = \{\boldsymbol{g}_1, \boldsymbol{g}_2, \cdots, \boldsymbol{g}_M\}$ can be computed using the following relation:

$$\boldsymbol{g}_m = \boldsymbol{b}_m \exp\{-\boldsymbol{A}_m \boldsymbol{f}\} \tag{1}$$

with $\boldsymbol{A}$ representing the forward projection operator. The X-ray source and the detector are mounted on a motorized computer-controlled arc. The entire assembly can be rotated along the arc, thereby allowing multiple acquisitions from different angles. We assume this rotation uniform and for each angular increment, the assembly rotates from $\Delta\theta$

$$\theta_m - \theta_{m-1} = \Delta\theta \tag{2}$$

Since the X-ray source is fixed with respect to the centre-of-rotation, the computation of each image projection for each rotation angle can be written under the following form:

$$\boldsymbol{g}_m = \boldsymbol{b}_m \exp\{-\boldsymbol{A}_0 \boldsymbol{Q}_\theta \boldsymbol{f}\} \tag{3}$$

with $\boldsymbol{Q}_\theta$ representing the rotation matrix. This latter one being block-diagonal, we can rewrite it in the following way:

$$\boldsymbol{Q}_\theta = diag\{\boldsymbol{q}_\theta, \boldsymbol{q}_\theta, \cdots, \boldsymbol{q}_\theta\} \tag{4}$$

With $\boldsymbol{q}_\theta$ the 2D rotation matrix associated with the projection to be computed for each θ rotation angle. This decomposition allows storing $\boldsymbol{A}_0$ and $\boldsymbol{q}_\theta$, providing thus an easy way to compute the projection matrix for both projection and back projection operations. Its size can thus be reduced by a ratio of 99.2%. Now if we consider only the symmetry property of $\boldsymbol{A}_0$, its storage will be limited to 25%.

TABLE I

CPU time costs (unit in second) of one Forward and Backward projection for a single angle = 0^o on a 2.5 GHz CPU and 4 GB memory storage. The interpolation method is distance driven[9], The mean gain achievable on the projection and back projection operations are approximately 25% and 10% respectively

Time cost for volume(256^3)	Forward Projection	Backward Projection
Without matrix pre-computation	1.23s	3.13s
With matrix pre-computation	0.32s	0.32s

B. ECG gating reconstruction

The image acquisition is performed in a short time period (maximum four cardiac cycles). Because of the motion, the number of projections, we can consider for the reconstruction, is small, equal to four. The images are known a priori to be sparse in the space domain. We thus investigated three regularized statistical iterative algorithms for the image reconstruction considering a Poisson model for data. We can thus define a MAP reconstruction for which we looked for minimizing the function:

$$\Phi(\boldsymbol{f}) = -L(\boldsymbol{g}|\boldsymbol{f}) + \beta R(\boldsymbol{f}) \tag{5}$$

With $\boldsymbol{g}$ representing the observed image, $L(\boldsymbol{g}|\boldsymbol{f})$ the Poisson log-likelihood function and $R(\boldsymbol{f})$ the image prior function known as a regularizer or a penalty.

$$L(\boldsymbol{g}|\boldsymbol{f}) = \sum_i \left(-\bar{g}_i + g_i \log(\bar{g}_i) - \log(g_i)\right) \tag{6}$$

with

$$\bar{g}_i \cong Poisson(\boldsymbol{g}_m)_i + r_i \tag{7}$$

We investigated three regularizer which are respectively L2, L1 and L0 norm prior in the EM algorithm as a sparsity measure. For L2 norm prior, the potential function is:

$$\varphi(t) = t^2 \tag{8}$$

and for L1 norm prior:

$$\varphi(t) = |t| \tag{9}$$

Unlike the L2 and L1 norm, the L0-norm is non convex and not continuous and uniform almost everywhere except zero. This brings difficulty for the optimization. We use a set of surrogate potential functions and gradually approximates the reconstructions by a set of outer iterations which was defined in this paper:

$$\varphi(t, \rho) = \frac{2}{\pi} \arctan\left(|t|/\rho\right) \tag{10}$$

By successively reducing ρ, the potential function approximates the definition of L0-norm:

$$\lim_{\rho \to 0} \varphi(t, \rho) = |\mathrm{sgn}(t)| \tag{11}$$

The use of (10) prevent the algorithm from falling into local minimal.

C. Optimization

The computation cost depends on two elements: the time cost per iteration and the convergence speed. The use of pre-computation matrix reduces the time cost per iteration. Besides this, we have to find an algorithm that provides a fast convergence. We choose the SPS algorithm introduced by Fessler for PET image reconstruction [10-11]. The key of the SPS method is to find a decomposition of the objective function (5) into quadratic surrogate functions to allow its minimization by a simple simultaneous update.

From (6), we can set the surrogate functions q_i under the following quadratic form:

$$q_i(g; g_i^n) = L_i(g_i^n) + \dot{L}_i(g_i^n)(g - g_i^n) + \frac{1}{2} c_i(g_i^n)(g - g_i^n)^2 \tag{12}$$

g_i^n denotes the estimate of the ith projection of the estimated image at the nth iteration. If $\dot{L}$ denotes the first derivative of L , we can set : $q_i(g_i^n; g_i^n) = L(g_i^n)$ and $\dot{q}_i(g_i^n; g_i^n) = \dot{L}(g_i^n)$. $c_i(g_i^n)$ characterizes the curvature of the parabola q_i satisfying:

$$L_i(g) \leq q_i(g; g_i^n), while g \geq 0 \tag{13}$$

The convergence speed depends on the curvature $c_i(g_i^n)$, whose definition was given by:

$$c_i(g_i^n) = \max \left\{ \begin{array}{cc} 2\frac{L_i(0)-L_i(g_i^n)+g_i^n \dot{L}_i(g_i^n)}{(g_i^n)^2} & \text{if } g_i^n > 0 \\ \ddot{L}_i(0) & \text{if } g_i^n = 0 \end{array} , 0 \right\} \quad (14)$$

The surrogate function can be set as follows:

$$Q(\boldsymbol{f}; \boldsymbol{f}^n) = \sum_i q_i(g_i; g_i^n) \quad (15)$$

A quadratic function applied at each pixel, is then given by:

$$\widehat{Q}_j^n(f_j) = Q(f_j^n; \boldsymbol{f}) + (f_j - f_j^n)\dot{Q}_j^n(f_j^n; \boldsymbol{f}) + \frac{1}{2} d_j^n (f_j - f_j^n)^2 \quad (16)$$

Where f_j^n is the current estimate of voxel f_j

$$\dot{Q}_j^n(f_j^n; \boldsymbol{f}) = \sum_i a_{ij} \dot{q}_i(g_i^n) \quad (17)$$

and

$$d_j^n = \sum_i a_{ij}^2 c_i(g_i^n) \quad (18)$$

To simplify the calculation, a pre-computation of d_j^n can be done as in [11]:

$$d_j^n = \sum_i a_{ij} \frac{(\bar{g}_i - r_i)^2}{\bar{g}_i} \left(\sum_j a_{ij} \right) \quad (19)$$

Since the potential function of L0-norm prior is not convex, it is difficult to generate a quadratic surrogate function. We separate thus the update into 2 parts:

$$\tilde{f}_j^{n+1} = \max(0, f_j^n - \frac{\dot{Q}_j^n(f_j^n)}{d_n^j}) \quad (20)$$

$$f_j^{n+1} = \max(0, \tilde{f}_j^{n+1} - \beta \dot{R}(f_j^n; \boldsymbol{f}^n, \rho)) \quad (21)$$

Finally, the algorithm is the following:

- Estimate background
- Initialize $\boldsymbol{f}^{\mathbf{o}}$, ρ^0, β^0,σ and ε
- For $k = 1, \cdots, K$, set $\rho = \rho^0 \delta^{(k-1)}$, $\beta = \beta^0 \varepsilon^{(k-1)}$
  - For $n = 1, \cdots, N$
    - For $\theta = \theta_1, \cdots, \theta_M$
      - Update $\hat{\boldsymbol{f}}^{n,m}$ estimation using (20) and (21)
      - Update forward projection $\boldsymbol{g}$ and $\dot{Q}^n$
- End

III. RESULTS

The experiments have been conducted on simulated data. These data were built from a 3D dynamic sequence acquired on a 64-slice GE LightSpeed CT coronary angiography[12]. A sequence of 20 3D binary coronary trees was built corresponding to 20 different cardiac phases. A C-arm rotational R-X coronary angiography was then simulated using the Siemens Axiom System imaging protocol. The detector plane $(200mm)^2$ was uniformly sampled into 512^2 pixels. Reconstructions were performed in a volume of $(110mm)^3$, 80 projections of the 3D binary tree were generated, uniformly spaced over the range RAO60^o to LAO60^o. 4 cardiac cycles were considered, this means that a volume (associated with a phase s of the cardiac cycle) was projected 4 times during the acquisition, according to different viewpoints. The projection operator A has been computed according to [9] and optimized according to section II.A. We used then the method of low order polynomials approximation to create the required background images from real angiography images acquired separately on the Siemens device (Fig. 1). Poisson noisy data were then generated, which were used for reconstructions.

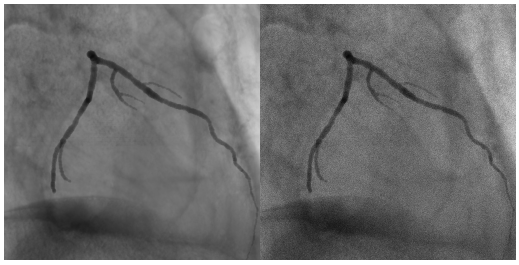

Fig. 1. Projection image acquired at angle RAO60^o: left: after background addition; right: after noise addition.

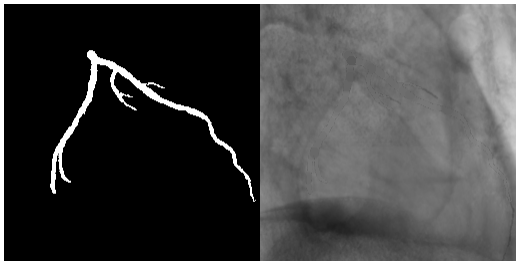

Fig. 2. Result of the background extraction: Left: vessel mask; right: estimated background image

A. Background Estimation

The background image, previously denoted $\boldsymbol{b}_m$, is unknown and was estimated from the projection data. We applied the following processing sequence:

- A low pass filtering on $\boldsymbol{g}$ (result noted ${}^1\boldsymbol{g}$)
- A top-hat filtering on ${}^1\boldsymbol{g}$ (result noted ${}^2\boldsymbol{g}$)
- A threshold on ${}^2\boldsymbol{g}$ (the result provides a vessel mask $\widetilde{\boldsymbol{g}}$)
- A Multiplication of the image g with the inverse mask:$\widetilde{\boldsymbol{g}}^{bkg} = \boldsymbol{g} \times (1 - \widetilde{\boldsymbol{g}})$
- A closing filtering on $\widetilde{\boldsymbol{g}}^{bkg}$

The final background image is then given by (Fig. 2): $\boldsymbol{g}^{bkg} = \widetilde{\boldsymbol{g}}^{bkg} \times \widetilde{\boldsymbol{g}} + \boldsymbol{g} \times (1 - \widetilde{\boldsymbol{g}})$

B. 3D Reconstruction

The 3D reconstruction was performed using the 3 regularizer: L2, L1 and L0 norm. The parameter β was chosen to minimize the MSE value of the reconstruction during iteration: β =0.2 for L2 norm and 0.02 for L1 norm. For L0 norm, we set $\rho^0 = 1.0$, $\sigma^0 = 0.7$, $\beta^0 = 1.0$ and $\varepsilon = 0.7$, $K = 8$, $N = 50$. For all the regularizers, the convergence was reached for 400 iterations. To evaluate the

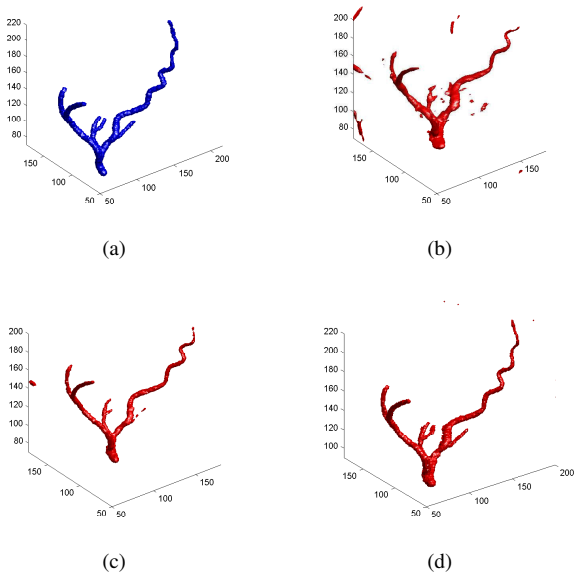

(a) (b) (c) (d)

Fig. 3. A result of the coronary reconstruction from 4 projections of phase 1(RAO 60^o, RAO 30^o, LAO 0^o, LAO 30^o) (a) original 3D coronary tree without the background, (b) reconstruction using L2 norm penalty (MSE 14.38%), (c) L1 norm (MSE 7.12%) (d) L0 norm (MSE 2.55%)

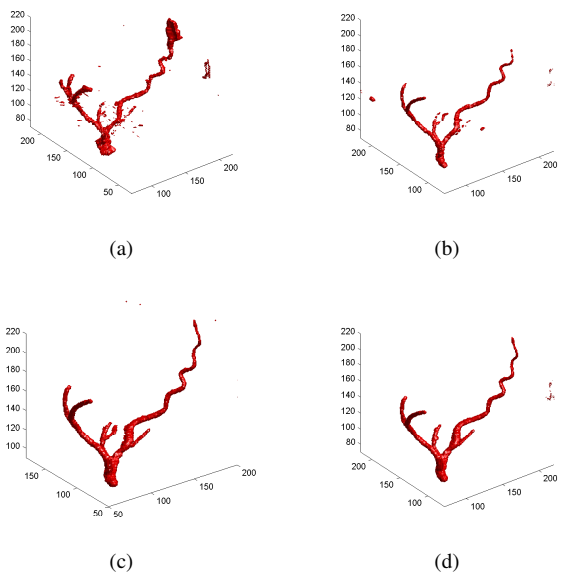

(a) (b) (c) (d)

Fig. 4. Influence of the relaxation value in the quality of the reconstruction: (a)σ= 0.5 (MSE:16.27%), (b)σ=0.6 (MSE :8.93%), (c)σ=0.7 (MSE: 2.55%) (d)σ=0.8 (MSE :4.35%)

results, we computed the normalized percentage error MSE (Fig.3).

Experiments showed that L0 norm prior provided the lowest MSE and the best quality of reconstruction. In the algorithm, a relaxation parameter σ was applied for successively approaching the "true L0 norm". Fig.4 shows the influence of this parameter in the reconstruction quality(σ sets in the range [0,1]). The chosen value was the one that minimized the MSE error. This value was found to be 0.7. Above, the reconstruction appears over smoothed with missing small branches. Under, artifacts appear due to the fact that the solution reaches a local minimum.

IV. CONCLUSION

We evaluated three penalized-likelihood algorithms for the 3D coronary artery reconstruction using a Poisson model for the data. Evaluations have been performed by means of a realistic phantom representing an arterial tree extracted from a sequence of MDCT datasets in order to get a ground truth. Results showed that L0-norm significantly improved the results compared to L1 and L2-norm. We also improved the global computation time of the reconstruction algorithm through the improvement of the time cost per iteration (in the projection-backprojection matrix computation) and the convergence speed of the algorithm.

V. ACKNOWLEDGMENTS

The authors thank Jian ZHOU for his contribution and his advices all along this research project

REFERENCES

[1] Schoonenberg G, Neubauer A., Grass M., Three-Dimensional coronary visualization, Part 2 : 3D reconstruction, Cardiology Clinics, *Advances in coronary Angiography*, vol. 27(3), 2009, pp 453-465.

[2] Rasche V, Movassaghi B, Grass M, et al. Automatic selection of the optimal cardiac phase for gated three-dimensional coronary X-ray angiography *Acad. Radiol.*, vol. 13, 2006, pp 630-640.

[3] Zhou J., Bousse A., Yang G., Bellanger J-J, Luo L., Toumoulin C., Coatrieux J.L, A blob-based tomographic reconstruction of 3D coronary trees from rotational X-ray angiography, *SPIE Medical imaging, San Diego, CA USA, 2008*, 2008, pp 6913-6924.

[4] Hansis E, Schafer D, Dossel O, et al. Evaluation of iterative sparse object reconstruction from few projections for rotational coronary angiography, *IEEE T-MI*, vol. 27(11), 2008, pp 1548-1555.

[5] Bousse A, Zhou A., Yang G, Bellanger J-J, Toumoulin C., Motion Compensated Tomographic Reconstruction of Coronary Arteries in Rotational Angiography, *IEEE T-BME*, vol. 56(4), 2009, pp 1254-1257.

[6] Blondel, G. Malandain, R. Vaillant, and N. Ayache, Reconstruction of coronary arteries from a single rotational X-ray projection sequence, *IEEE T-MI*, vol. 25, 2006, pp 653-663.

[7] Schafer D, Borgert J, Rasche V, et al. Motion compensated and gated cone beam filtered backprojection for 3D rotational angiography., *IEEE T-MI*, vol. 25(7), 2006, pp 898-906.

[8] Rohkohl C., Lauritsch G., Prmmer R.,Hornegger J., Interventional 4-D Motion Estimation and Reconstruction of Cardiac Vasculature without Motion Periodicity Assumption, *Springer-Verlag Berlin Heidelberg, MICCAI 2009*, Part I, LNCS 5761, 2009, pp 132-139.

[9] Man B. D. and Basu S., Distance-driven projection and backprojection in three dimensions, *Phys. Med. Biol.*, vol. 49, 2004, pp 2463-2475.

[10] Fessler J.A., Erdogan H., A paraboloidal surrogates algorithm for convergent penalized-likelihood emission image reconstruction., *In Proc. IEEE Nuc. Sci. Symp. Med. Im. Conf, 2, 1998*, 1998, pp 1132-1135.

[11] Erdogan H., Fessler J.A., Monotonic algorithms for transmission tomography, *IEEE T-MI*, vol. 18(9), 1999, pp 801-814.

[12] Yang G., Bousse A, Toumoulin C., and Shu H., A multiscale tracking algorithm for the coronary extraction in MSCT angiography, *in Proc Eng. Med. Biol. Soc. (EMBS)*, vol. 1, 2006, pp 3066-3069.